The EMPIR initiative is co-funded by the European Union's Horizon 2020 research and innovation programme and the EMPIR Participating States

EMPIR Project – JRP-n08: Sulf-Norm

WP2 A2.2.12

Modelling of SO_2 losses in conditioned sampling

Stanislav Knotek

Czech Metrology Institute

1 Introduction

This report presents the modeling of SO_2 diffusion into water droplet and water film which arise in P-AMSs during the process of drying. The motivation is an attempt to quantify the SO_2 losses in dryers during sampling of emissions.

Two basic phenomena need to be taken into account in modeling of removing gaseous substances during drying process. Since the gas is dissolved in liquid water condensing in the dryer, the condensation processes are needed to be described quantitatively in dependence on the physical and geometrical conditions. Once the microscopic liquid phase of water occurs in the dryer (in form of water film or water droplet), the transfer of gaseous soluble species into water is driven by diffusion processes simultaneously with the ongoing condensation of water. Thus, the condensation and diffusion are the key physical phenomena needed to model. However, in more detailed view, the mechanism of dissolution of gaseous substances into liquid consists of four partial processes:

a) transport of molecules in the gas phase towards the liquid surface (convection, diffusion, Stephan's flow)

b) transport of the molecules across the gas-liquid interface (mass accommodation effect, Henry's law)

c) transport of molecules in the liquid phase (convection, diffusion)

d) chemical reactions in the liquid phase

Since the condensation of water is supposed, the studied situation is moreover complicated by

e) growth of the water droplet or liquid film formation

All of these phenomena are needed to be implemented in the mathematical model. On top of that, since the processes are running simultaneously, the coupled solution is needed. The mathematical description of each phenomena will be outlined in section 2 and the resulting coupled solution of the comprehensive model will be presented in section 3.

2 Theoretical backgrounds

2.1 Initial assumptions

For the theoretical findings outlined in the next paragraphs, the single spherical droplet is supposed to be located in mixture of humid air and gaseous SO_2. For simplicity, the following other assumptions are taken into account for description of condensing droplet:

i. The convection in the droplet and Stefan's flow near the droplet surface due to vapor condensation are not considered.

ii. No other soluble species than SO_2 are supposed. Note that especially in case of salt water vapor the influence on droplet growth should be assessed.

iii. The heat transfer is not modeled in gas phase nor in liquid phase. According to [1] under the conditions of slow growth, the droplet temperature is approximately the same as the ambient temperature. In case of more rapid growth empirical relation for droplet temperature based on ambient temperature and relative humidity can be used, see bellow in paragraph 2.2.

iv. The molar volume of the SO_2 dissolved in water is negligible, thus the droplet growth is caused only be condensation of water vapor.

v. At the droplet surface the equilibrium state of water vapor is supposed, thus the partial water vapor pressure is given by the saturation pressure at the droplet (surface) temperature.

vi. Since the volume concentration of SO_2 is low, the latent heat of SO_2 is negligible compared with the heat released by water vapor condensation.

Analogical assumptions are valid for condensing of liquid film and two others are supposed:

vii. The liquid film can be considered as planar.

viii. The laminar convection in the liquid film and the gas phase is taken into account.

On top of assumptions just mentioned, the scheme of the dryer is supposed to be simplified according to Figure 1.

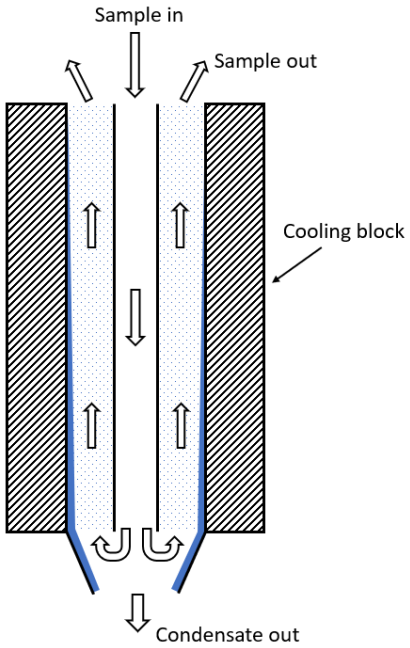

Figure 1: Scheme of the condensation in dryer.

In the following text, the theoretical findings for phenomena a) – e) assuming i. – viii. are presented according to cited references.

2.2 Droplet growth by condensation

For the description of the droplet growth, the book [1] can serve as a good source text and support the following paragraphs.

The condensation processes in humid air depends on the saturation ratio (multiplied by 100% known as relative humidity) of the partial pressure of water vapor to the saturation vapor pressure

$$S_R = \frac{p}{p_s} \tag{1}$$

The saturation water vapor pressure for a plane liquid surface is given by empirical formula

$$p_s = \exp\left(16.7 - \frac{4060}{T - 37}\right) \tag{2}$$

where T is the absolute temperature in K and p_s is the saturation pressure in kPa. In case of the plate surface water begin to condense if $S_R = 1$. However, the saturation ratio, called the Kelvin ratio K_R, in case of microscopic water droplets is given by the Kelvin or Thomson-Gibbs equation

$$K_R = \frac{p_d}{p_s} = \exp\left(\frac{4\gamma M}{\rho R T d}\right) \tag{3}$$

where γ, M, ρ and R are the surface tension, molecular weight, density of the liquid and universal gas constant, respectively, p_d is partial pressure at the surface of the droplet with diameter d.

Once a stable nucleus of droplet is established, i.e. the diameter of nucleus is bigger than d given by formula (3) for a given saturation ratio (or reversely saturation ratio is bigger than K_R given by formula (3) for a given nucleus diameter), the droplet begins to growth. In [1] two formula in dependence on the current diameter are derived. When the droplet diameter is less than gas mean free path, λ, the formula has the form

$$\frac{\mathrm{d}(d_p)}{\mathrm{d}t} = \frac{2M\alpha(p_\infty - p_d)}{\rho N_A \sqrt{2\pi m k T}} \qquad \text{for } d_p < \lambda \tag{4}$$

where α is accommodation coefficient, see the section 2.4, p_∞ is partial pressure far from the droplet surface, p_d is partial pressure of vapor at the droplet surface given by Kelvin equation (3), N_A is Avogadro constant, $m = M/N_A$ is mass of vapor molecule and $k = 1.3806485 \cdot 10^{-23}$ is Boltzmann constant.

In case the droplet is bigger than mean free path, the formula becomes

$$\frac{\mathrm{d}(d_p)}{\mathrm{d}t} = \frac{4DM}{R\rho d_p}\left(\frac{p_\infty}{T_\infty} - \frac{p_d}{T_d}\right)\phi \qquad \text{for } d_p > \lambda \tag{5}$$

where D is diffusion coefficient of water vapor, ϕ is the Fuchs correction factor significant for particles less than 1μm, p_d is vapor partial pressure near the droplet surface which according to assumption v. can be calculated by formula (2) and finally the droplet temperature T_d can be computed using ambient temperature T_∞ by

$$T_d = T_\infty + \frac{(6.65 + 0.345T_\infty + 0.0031T_\infty^2)(S_R - 1)}{1 + (0.082 + 0.00782T_\infty)SR} \tag{6}$$

where T_∞ in ratio needs to be in °C.

Since gas mean free path is quite small in comparison to final droplet diameters, the amount of dissolved SO_2 is not affected by the initial droplet growth described by (4). Moreover, since the expected final droplet diameters are much bigger than 1 µm (due to filter resolution), the droplet growth can be approximated by equation (5) for $\phi = 1$. After integration of (5) we get the prescription for droplet diameter in time by

$$d_p(t) = \sqrt{\frac{8DM}{R\rho}\left(\frac{p_\infty}{T_\infty} - \frac{p_d}{T_d}\right)(t - t^0) + \left(d_p^0\right)^2} \tag{7}$$

where d_p^0 is initial droplet diameter in time t^0.

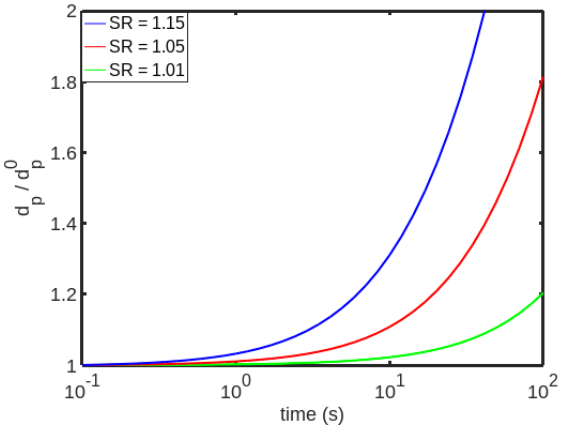

Figure 2: Temporal evolution of the droplet diameter in dependence on the saturation ratio.

2.3 Liquid film condensation

The classical analysis of laminar film on inclined or vertical wall is known from Nusselt (1916). Since the film covers whole surface, the condensation process is pushed by the heat transfer between the vapor and wall. Following from the Fourier's Law and supposing some assumptions (laminar flow, stagnant liquid vapor, smooth liquid film surface, etc. see [2]), the following formula (8) for liquid film thickness, δ, can be derived.

$$\delta(x) = \left(\frac{4k_l\mu_l x\Delta T}{\rho_l(\rho_l - \rho_v)gh_{lv}}\right)^{1/4} \tag{8}$$

where k_l is thermal conductivity of the liquid, μ_l and ρ_l are dynamic liquid viscosity and liquid density, ρ_v is vapor density, x is coordinate in the wall direction and h_{lv} is latent heat of the liquid-vapor phase change.

As follows from the design of P-AMSs, the film is supposed to flow downward due to gravity, while stack gas is flowing upward through the cooler. We speak about countercurrent vapor flow and the motion of gas needs to be taken into account. Authors in [2] show that a nonlinear system of govern-

ing equations is derived if a shear stress from vapor motion is supposed on the liquid film interface. The corresponding mechanistic models are outlined in [3], [4] or [5]. Numerical implementation using finite volume methods can be found in [6] or [7]. However, since the models of countercurrent are rather complex, the film thickness given by Nusselt theory is taken as the acceptable estimate.

2.4 Mass transfer through gas-liquid interface

Henry's law

The basic form of Henry's law says that the concentration of a species in the aqueous phase, n_l, is proportional to the partial pressure of this matter in the gas phase, p, according to formula

$$n_l = H^{cp}\, p \tag{9}$$

where H^{cp} is the Henry's law constant in mol·m^{-3}·Pa^{-1}. Note that there are several other definitions of Henry's law constant. The dimensionless form is given by

$$H^{cc} = \frac{n_l}{n_g} \tag{10}$$

The conversion between H^{cp} and H^{cp} for ideal gas is

$$H^{cc} = H^{cp} R\, T \tag{11}$$

where R is the universal gas constant.

The dependence of Henry's law constant on temperature can be extrapolated from a single data point applying van't Hoff equation by formula

$$H(T) = H^0 \exp\left[-\frac{\Delta h}{R}\left(\frac{1}{T} - \frac{1}{T^0}\right)\right] \tag{12}$$

where H^0 is Henry's law constant in temperature T^0 and Δh is enthalpy change due to transport of soluble gas substance into liquid. The dependence of Henry's law constant on temperature and independence on pressure have been confirmed in [8]. The values of Henry's law constant for different substances and water as solvent can be found in [9]. Selected values of H^0 and $-\Delta h/R$ can be found in Table 1 for T^0=298.15 K. The corresponding Henry's constants in dependence on temperature are depicted in Figure 3.

Table 1: Parameters for determination of Henry's Law constant according to formula (8).

H^{cp} at T^0 (mol m^{-3} Pa^{-1})	$\frac{\mathrm{d}\ln H^{cp}}{\mathrm{d}(1/T)}$ (K)	Reference
1.4·10^{-2}	2800	[10]
1.2·10^{-2}	3200	[11]
1.3512·10^{-2}	3715.2	[12]
1.3·10^{-2}	2900	[13]

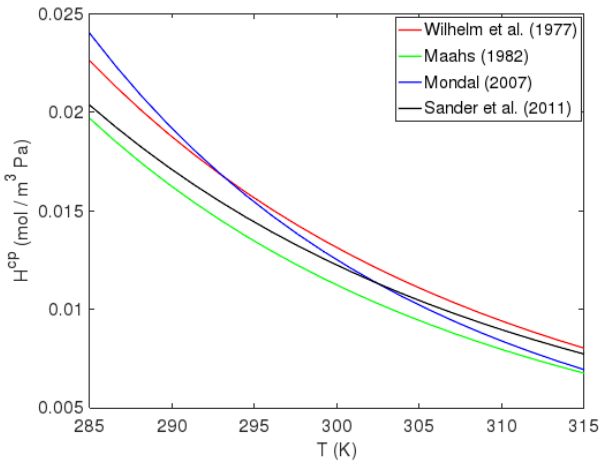

Figure 3: Henry's Law constant vs. temperature.

Mass accommodation coefficient (sticking coefficient)

The mass accommodation coefficient, α, is defined as the ratio of molecules absorbed through the gas-liquid interface to the number of molecules which hit the liquid surface. As has been shown in [14] using the comparison of characteristic times of different processes, the droplet surface is saturated faster than equilibrium state can be established due to diffusion. This leads to the re-evaporation of some molecules from interface and the resulting ratio of absorbed molecules can be described using the mass accommodation coefficient. The experimental measurements of mass accommodation coefficient of SO_2 at the air-water interface are presented in [14] and [15]. The authors report measurements of $\alpha = (6.0 \pm 0.8) \cdot 10^{-2}$ at 298 K and $\alpha = (5.4 \pm 0.6) \cdot 10^{-2}$ at 295 K, respectively.

2.5 Physical and chemical processes in liquid phase

Chemical reactions

Experimental observations in [14] show that the mass accommodation coefficient is strongly dependent on pH and real solubility at the droplet surface. For considering of these dependencies, the chemical processes in droplet need to be take into account. According to [16], the following chemical reactions occur if SO_2 is dissolved in water

$$\mathrm{SO_2(g) + H_2O} \xrightarrow{K_H} \mathrm{SO_2 \cdot H_2O}\,, \qquad K_H = \frac{[\mathrm{SO_2 \cdot H_2O}]}{p_{\mathrm{SO_2}}} \tag{13}$$

$$\mathrm{SO_2 \cdot H_2O} \xrightarrow{K_1} \mathrm{H^+ + HSO_3^-}\,, \qquad K_1 = \frac{[\mathrm{H^+}][\mathrm{HSO_3^-}]}{[\mathrm{SO_2 \cdot H_2O}]} \tag{14}$$

$$\mathrm{HSO_3^-} \xrightarrow{K_2} \mathrm{H^+ + SO_3^{2-}}\,, \qquad K_2 = \frac{[\mathrm{H^+}][\mathrm{SO_3^{2-}}]}{[\mathrm{HSO_3^-}]} \tag{15}$$

where [·] represents the concentration, K_H is the Henry's constant H^{cp}, K_1 and K_2 are the first and the second dissociation constants. The total concentration of the dissolved sulfur with oxidation number four can be calculated as the sum

$$[S(IV)] = [\mathrm{SO_2 \cdot H_2O}] + [\mathrm{HSO_3^-}] + [\mathrm{SO_3^{2-}}] \tag{16}$$

Expressing (16) using dissociation constants defined in (13-15), the total concentration has form

$$[S(IV)] = K_H\, p_{\mathrm{SO_2}} \left(1 + \frac{K_1}{[\mathrm{H^+}]} + \frac{K_1\, K_2}{[\mathrm{H^+}]^2}\right) \tag{17}$$

Effective Henry's constant

Following the considerations in previous paragraph, the equilibrium state of the sulfur dioxide concentration inside the droplet can be expressed by

$$n_l = H_{S(IV)}^{cp,*} p_{\mathrm{SO_2}}\,, \tag{18}$$

where $H_{SO_2}^{cp,*}$ is the effective Henry's constant. Using (17) the effective Henry's constant has the form

$$H_{S(IV)}^{cp,*} = K_H \left(1 + \frac{K_1}{[\mathrm{H^+}]} + \frac{K_1 K_2}{[\mathrm{H^+}]^2}\right), \tag{19}$$

where concentration [H⁺] is connected with pH scale by

$$\mathrm{pH} = -\log[\mathrm{H^+}]\,, \tag{20}$$

where [H⁺] need to be in mol/dm³.

Note that neglecting the second dissociation term $[\mathrm{SO_3^{2-}}]$ which has very low concentration and using equality $[\mathrm{H^+}] = [\mathrm{HSO_3^-}]$, see [12], the effective Henry's law constant can be expressed by

$$H_{S(IV)}^{cp,*} = K_H + \sqrt{\frac{K_H K_1}{p_{\mathrm{SO_2}}}} \tag{21}$$

As well as the Henry's law constant also the dissociation constants are dependent on temperature. According to experimental data between 0 and 50°C author in [11] proposed correlations

$$\log K_1 = \frac{853}{T} - 4.74 \tag{22}$$

$$\log K_2 = \frac{621.9}{T} - 9.278 \tag{23}$$

Measurements based formula for K_1 in mol/dm³ presents [12] using

$$\ln K_1 = \frac{1447.1}{T} - 9.11 \tag{24}$$

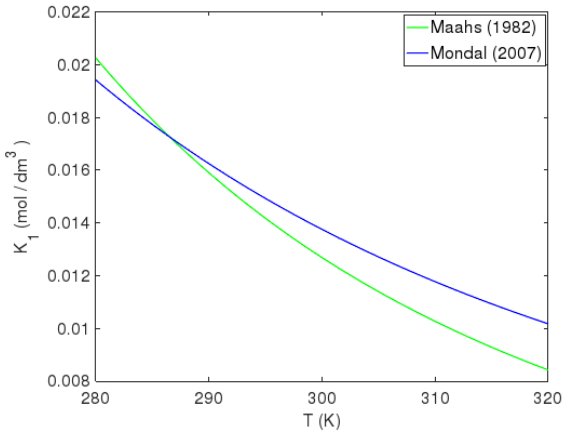

Figure 4: First dissociation constant K_1 vs. temperature.

Using equations (18) and (21), prescription for Henry's constant K_H from [12], see Table 1, and prescription for K_1 by formula (24) authors in [12] derived equation for total concentration of sulfur dioxide absorbed in water in dependence on temperature

$$[S(IV)] = 2.407 \cdot 10^{-6} \cdot \left[0.0218 \cdot \exp\left(\frac{3715.2}{T}\right) p + \exp\left(\frac{2581.1}{T}\right) p^{0.5}\right] \tag{25}$$

where $[S(IV)]$ is in mol/dm^3 , T in K and p in kPa. The corresponding concentration of SO_2 which can be absorbed from air with initial concentration of 0.01 ppm in dependence on temperature can be seen in Figure 5.

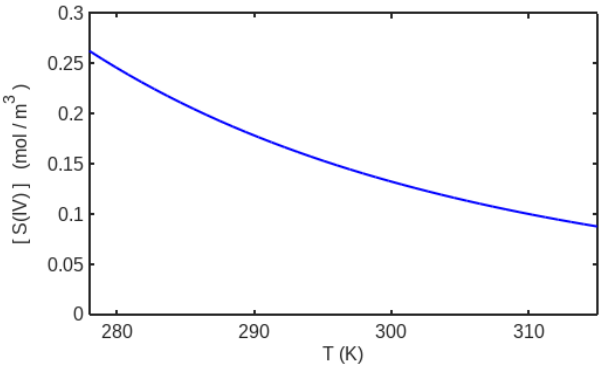

Figure 5: Total SO_2 absorbed in water in dependence on temperature. Initial SO_2 concentration in air 0.01ppm.

2.6 Diffusion

Governing equations

The diffusion processes are described by equation

$$\frac{\partial n(x,t)}{\partial t} = \frac{\partial}{\partial x}\left(D \frac{\partial n(x,t)}{\partial x}\right) \tag{26}$$

where $n(x,t)$ is concentration in position x and time t and D is the diffusion coefficient. As was already mentioned in introduction, the studied phenomenon need to be solved as coupled system

for both phases, therefore the system of two coupled diffusion equation for constant diffusion coefficients takes the form

$$\frac{\partial n_g(x,t)}{\partial t} = D_g \frac{\partial^2 n_g(x,t)}{\partial x^2} \tag{27}$$

$$\frac{\partial n_l(x,t)}{\partial t} = D_l \frac{\partial^2 n_l(x,t)}{\partial x^2} \tag{28}$$

The dependence of diffusion coefficient of SO_2 in water on temperature and pH is presented in [17]. The influence on temperature is given by

$$D_l = -1.21 \cdot 1010^{-3} + 4.33 \cdot 10^{-6} \cdot T \tag{29}$$

Initial conditions define the concentrations inside and outside of the droplet:

$$n_l(x,0) = n_{l,0} \qquad \text{for x} < d_p/2 \tag{30}$$

$$n_g(x,0) = n_{g,0} \qquad \text{for } x > d_p/2 \tag{31}$$

Since the concentration far from the surface is supposed to be constant, the mass flux due to diffusion vanishes. Similarly, the mas flux can be assumed to be zero at the centre of droplet due to symmetry of the process. The corresponding boundary conditions can be defined as

$$-D_l \frac{\partial}{\partial x} n_l(0,t) = n_{l,0} \tag{32}$$

$$-D_g \frac{\partial}{\partial x} n_g(\infty,t) = n_{g,0} \tag{33}$$

Analytical solutions of equations (27) and (28) for different geometrical configurations and different boundary conditions are given in [18]. However, the presented suitable solutions do not take into account the Henry's law which limits the maximal concentration of dissolved substance in liquid and the mass accommodation coefficient which defines the fraction of molecules entering through the gas-liquid interface.

Boundary conditions at the interface

The boundary conditions which take into account the Henry's Law and accommodation coefficient are presented in [19] by forms

$$-D_g \frac{\partial}{\partial x} n_g(d_p/2,t) = \frac{\alpha\, \bar{v}}{4}\left(n_g(d_p/2,t) - \frac{n_l(d_p/2,t)}{H^{cc}}\right), \tag{34}$$

$$-D_l \frac{\partial}{\partial x} n_l(d_p/2,t) = \frac{\alpha\, \bar{v}}{4}\left(n_g(d_p/2,t) - \frac{n_l(d_p/2,t)}{H^{cc}}\right), \tag{35}$$

where the gas-liquid interface is located at x=$d_p/2$ and $\bar{v}$=300 m/s is mean thermal velocity of SO_2 as given by [20].

3 Numerical model and results

Fairly comprehensive attitude to the modeling of soluble gas transport into large droplets during evaporation and condensation is presented in [16] and [21]. Rather complex numerical solution of the presented partial differential equations with moving boundaries led to the idea of using the tool based on finite element (FEM) or finite volume method (FVM).

Regarding to the geometry and physical configuration of the supposed dryer, the estimate of maximal concentrations can be done separately using model of diffusion into the growing droplet and into the condensing film.

In case of droplet, simultaneous simulation of diffusion and droplet growth need to be done. Resulting concentrations inside droplet computed using FEM tool are presented in Figures 6 in dependence on time and initial SO_2 concentrations. The model is based on equations (27-28) with initial conditions for gas and liquid (32-33) and boundary conditions (34-35) prescribed on gas-liquid interface. The mass accommodation coefficient is set to 0.054, the effective Henry's law constant is computed using (21) where dissociation constants K_H and K_1 are taken from [12], see Table 1 and formula (24) . The droplet growth is defined by formula (7) where droplet temperature is prescribed by formula (6), vapor partial pressure is given by equation (3) and saturation pressure is given by (2).

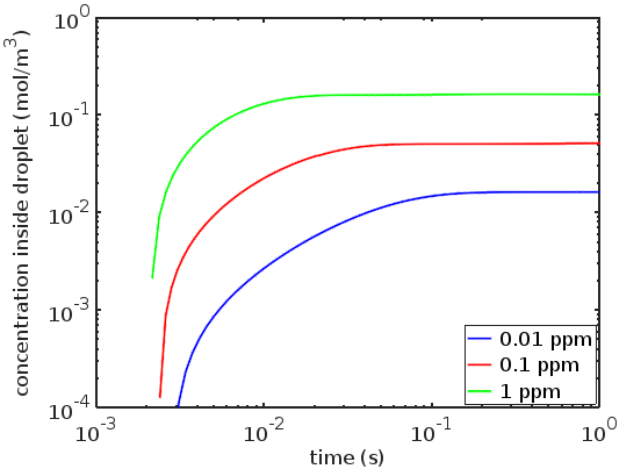

Figure 6: Concentration of SO2 in growing droplet during time for different values of SO2 concentration in air with relative humidity equal to 101% and temperature 20°C.

The Figure 6 shows the concentration of SO_2 in growing droplet in dependence on time. Depending on the initial concentration of SO_2 in gas, the time needed to reach the maximal concentration, which is given by formula (25), ranges between 0.02 and 0.2s. Regarding the dimensions of condensation tubes in P-AMSs (diameter of the tube from 6mm, height from 125 mm) and maximal flow velocity of sampled air (approx. 0.4 m/s) , we can suppose, that the maximal concentration can be reached before the droplet is attached to the liquid film on the wall. On the other hand, the droplets are established only in case the relative humidity is bigger than 100%. In other cases, the condensation on the cooled wall with temperature 5°C is predominant for the drying processes in the dryer. Hence, the modeling of liquid film formation due to condensation and corresponding SO_2 dissolution is important for total amount of dissolved SO_2.

In contrast to the growing droplet, in case of the condensing liquid film, the corresponding analysis can be done for a given film thickness, if we can suppose that in process of measurement a stagnant liquid film is established. However, although the stationary liquid film thickness can be taken into account, note that the mathematical models suffer from other complications such as the modeling of interfacial friction or liquid velocity on the film surface in case of moving vapor in dryer when the formula (8) cannot be used.

In case of a typical P-AMS, the maximum gas volume flow rate is 150 Nl/h. For a tube with diameter 6mm, this corresponds to gas velocity of about 0.4m/s and laminar flow regime. Supposing limited influence of this laminar flow on the liquid film, the classical Nusselt formula (8) can serve as a basic estimate of the liquid film thickness along the dryer and the liquid volume in which the gas can diffuse. Supposing the length of the dryer tube 0.15m with diameter 0.006m and standard physical properties of water, the film thickness using (8) equals about 0.1 mm for saturation temperature of about 290K. As in the case of water droplet, several FEM simulations have been done using the theoretical basis outlined in the previous chapter. The main difference was the stagnant interface between liquid and gas phase and resolution of convection using the assumptions of laminar flow regimes in both phases. The constant film thickness of 0.1mm has been defined along the 0.15m long dryer. Zero flux of SO_2 has been prescribed in the upper boundary of liquid film and on the wall. The boundary conditions (34-35) have been prescribed on the gas-liquid interface.

The resulting concentration field of SO_2 in stack gas inside the dryer is depicted in Figure 7.

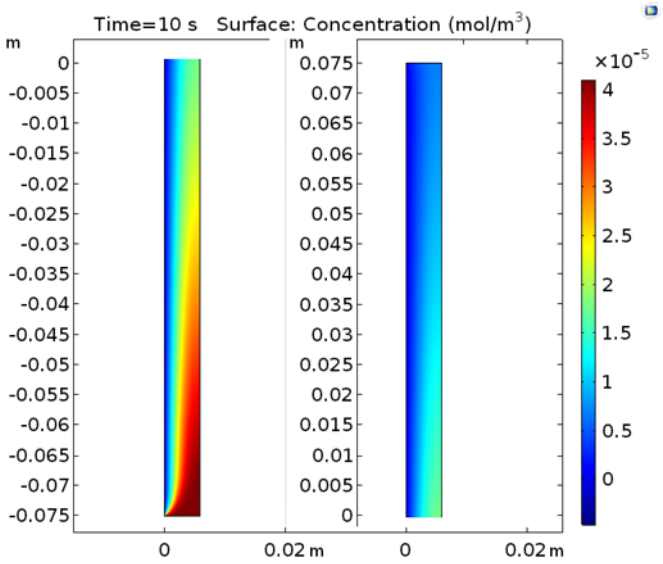

Figure 7: Concentration of SO2 in gas inside dryer in time 10s for initial SO2 concentration 1ppm and gas velocity 0.1 m/s.

The resulting ratios of outlet to inlet SO_2 concentrations in gas for different average velocity of gas flow and different inlet concentrations can be read in Table 2. The resulting dependencies show that SO_2 losses increase with decreasing gas velocity and decreasing SO_2 concentration in gas phase. The losses increase only slightly for lower inlet concentrations, while dependence on the gas velocity is much more significant.

Table 2: SO_2 concentration after passing through the cooler with constant water film thickness. Resulting values are normalized to the initial concentration before entrance to the cooler.

	n_g^{SO2} =1 ppm	n_g^{SO2} =10ppm	n_g^{SO2} =100ppm
U_g = 0.4 m/s	46.9 %	48.4 %	52.4 %
U_g = 0.2 m/s	28.6 %	29.9 %	33.8 %
U_g = 0.1 m/s	12.6 %	13.4 %	16.0 %

4 Conclusions

The presented mathematical models of droplet growing and liquid film formation during condensation have been outlined on basis of theoretical as well as experimental findings published in literature. The molecular transport of condensable gas is modeled with regards to the molecular processes on gas-liquid interface as well as with regards to chemical processes inside liquid. The governing equations of diffusion processes are solved using boundary condition on gas-liquid interface which is designed using physical parameters mentioned in theoretical sections.

The concentrations of SO_2 dissolved in one droplet needs to be computed using presented mathematical model of diffusion simultaneously with modeling of droplet growth. From the comparison of droplet growth time and droplet lifetime (time needed for leaving of the droplet from the dryer) it follows that ratio of final and initial droplet diameter is less than two. Thus, the dissolution of SO_2 into droplets should be less significant than dissolution into water film and therefore in following computations, summarized in Table 2, only liquid film condensation has been taken into account.

The average concentration of SO_2 in gas flow leaving the dryer has been simulated for stagnant film thickness, but as well as for droplet using aforementioned diffusion model based on Henry's law theory and chemical reactions connected with dissolution of SO_2 in water. From the comparison of resulting SO_2 concentrations at the inlet to the dryer and the final concentrations at the outlet from the dryer it follows that the SO_2 losses can be significant for the measurements using P-AMSs.

4.1 Summary of simplifications and challenges for future

In addition to basic assumptions outlined in section 2.1, following simplifications and notes need to be taken into account for assessing of model relevance in qualitative and quantitative sense:

- Only 2D simplified geometry, see Figure 1, with given dimensions (diameter D=6mm, height L=15cm) has been used for computations of SO_2 diffusion into water film condensed in dryer.
- The water film thickness has been set to constant value t=0.1mm according to formula (8).
- Constant temperature of stack gas, T_∞, and water film, T_w, has been set (T_∞=20°C, T_w=5°C).
- Relative humidity has been set to 101%.

- Better modeling of the film thickness for countercurrent vapor flow is needed.
- Initial gas properties (temperature, humidity) should be set according to real values.
- Adjustment of parameters and validation using real process or experiments is needed.

References

[1] W. C. Hinds, Aerosol Technology, New York: John Wiley & Sons, Inc., 1999.

[2] A. Faghri and Y. Zhang, Transport Phenomena in Multiphase Systems, London: Academic Press, Elsevier Inc., 2006.

[3] A. Faghri, "Turbulent Film Condensation in a Tube with Concurrent and Countercurrent Vapor Flow," in *AIAA/ASME 4th Joint Thermophysics and Heat Transfer Conference*, Boston, 1986.

[4] S. Thumm, C. Philipp and U. Gross, "Film condensation of water in a vertical tube with countercurrent vapour flow," *International Journal of Heat and Mass Transfer 44,* pp. 4245-4256, 2001.

[5] R. A. Seban and J. A. Hodgson, "Laminar film condensation in a tube with upward vapor flow," *International Journal of Heat and Mass Transfer, Vol. 25, No. 9,* pp. 1291-1300, 1982.

[6] N. Samkhaniani and M. R. Ansari, "The evaluation of the diffuse interface method for phase change simulations using OpenFOAM," *Heat transfer - Asian Res,* pp. 1-31, 2017.

[7] M. K. Groff, S. J. Ormiston and H. M. Soliman, "Numerical solution of film condensation from turbulent flow of vapor-gas mixtures in vertical tubes," *International Journal of Heat and Mass Transfer, 50,* pp. 3899-3912, 2007.

[8] N. Zhang, J. Zhang, Y. Zhang, J. Bai and X. Wei, "Solubility and Henry's law constant of sulfur dioxide in aqueous polyethylene glycol 300 solution at different temperatures ans pressures," *Fluid Phase Equilibria, 348,* pp. 9-16, 2013.

[9] R. Sander, "Compilation of Henry's law constants (version 4.0) for water as solvent," *Atmospheric Chemistry and Physics, 15,* pp. 4399-4981, 2015.

[10] E. Wilhelm, R. Battino and R. J. Wilcock, "Low-pressure solubilty of gases in liquid water," *Chem. Revi., 77,* pp. 219-262, 1977.

[11] H. G. Maahs, "Sulfur-dioxide/water equilibria between 0° and 50°C. An examination of data at low concentrations," in *Heterogeneous Atmospheric Chemistry, Geophysical Monograph, 26*, S. D. R., Ed., Washington, D.C., Am. Geophys. Union, 1982, pp. 187-195.

[12] M. K. Mondal, "Experimental determination of dissociation constant, Henry's constant, heat of reactions, SO2 absorbed and gas bubble-liquid interfacial area for dilute sulphur dioxide

absorption into water," *Fluid Phase Equilibria, 253,* pp. 98-107, 2007.

[13] S. P. Sander, J. Abbat, J. R. Barker, J. B. Burkholder, R. R. Friedl, D. M. Golden, R. E. Huie, C. E. Kolb, M. J. Kurylo, G. K. Moortgat, V. L. Orkin and P. H. Wine, "Chemical Kinetics and Photochemical Data for Use in Atmospheric Studies, Evaluation No. 17, JPL Publication 10-6, Jet Propulsion Laboratory, Pasadena," 2011. [Online]. Available: http://jpldataeval.jpl.nasa.gov.

[14] J. L. Ponche, C. George and P. Mirabel, "Mass Transfer at the Air/Water Interfrace: Mass Accommodation Coefficients of SO2, HNO3, NO2 and NH3," *Journal of Atmospheric Chemistry, 16,* pp. 1-21, 1993.

[15] J. A. Gardner, L. R. Watson, Y. G. Adewuyi, P. Davidovits, M. S. Zahniser, D. R. Worsnop and C. E. Kolb, "Measurement of the Mass Accommodation Coefficient of SO2 (g) on Water Droplets," *Journal of Geophysical Research, vol. 92, No. D9,* pp. 10887-10895, 20 September 1987.

[16] T. Elperin, A. Fominykh and B. Krasovitov, "Scavenging of soluble gases by evaporating and growing cloud droplets in the presence of aqueous-phase dissociation reaction," *Atmospheric Environment, 42,* pp. 3076-3086, 2008.

[17] A. Koliadima, J. Kapalos and L. Farmakis, "Diffusion Coefficients of SO2 in Water and Partition Coeffiecient of SO2 in Water-Air Interface at Different Temperature and pH Values," *Instrumentation Science & Technology, 37:3,* pp. 274-283, 21 April 2009.

[18] J. Crank, The Mathematics of Diffussion, Oxford: Clarendon Press, 1975.

[19] T. Huthwelker and T. Peter, "Analytical description of gas transport across an interface with coupled diffusion in two phases," *J. Chem. Phys, 105, (4),* pp. 1661-1667, 22 July 1996.

[20] J. O. Hirschfelder, C. F. Curtiss and R. B. Bird, Molecular Theory of Gases and Liquids, New York: Wiley, 1954.

[21] T. Elperin, A. Fominykh and B. Krasovitov, "Evaporation and Condensation of Large Droplets in the Presence of Inert Admixtures Containing Soluble Gas," *Journal of the Atmospheric Sciences,* pp. 983-995, March 2007.